coatings

MDPI

Article

Research on Low-Brightness and High-Reflective Coatings Suitable for Buildings in Tropical Areas

Xian Rong [1], Lichao Jiao [1,2,*], Xiangfei Kong [3] and Guangpu Yuan [3]

1 School of Civil and Transportation Engineering, Hebei University of Technology, Tianjin 300401, China; xianrong2016@sohu.com
2 School of Management, Henan University of Urban Construction, Pingdingshan 467036, China
3 School of Energy and Environmental Engineering, Hebei University of Technology, Tianjin 300401, China; beijingxinyong16_1@163.com (X.K.); guangpu2020@126.com (G.Y.)
* Correspondence: 201611601006@stu.hebut.edu.cn or jiaolichao2006@126.com; Tel.: +86-18222768286

Received: 22 July 2020; Accepted: 25 August 2020; Published: 27 August 2020

Abstract: In this article, we mixed hollow glass beads with nano-TiO_2 and iron oxide red in a certain proportion to prepare a low-brightness, high-reflective, safe, and durable cooling coating throughout the experiments. The coating is suitable for energy-saving in tropical areas. To discuss the energy saving effects of the coating on an exterior envelope in tropical areas, a comparative analysis for two scenario models of a two-story residential building in Kuala Lumpur, Malaysia was conducted. The results indicated that the heat reflective insulation coating could reduce the exterior envelope surface temperature effectively, and the maximum temperature change was about 6–8 °C. Through calculations, it was found that the annual energy saving rate was 12.9%, which showed that the energy saving effect of the heat insulation coating was obvious in Kuala Lumpur. The brightness of the coating was less than 50%, and its comfort and safety met the requirements.

Keywords: tropical climate; low brightness; high reflection; hollow glass beads; nano-coating; thermal characteristics; orthogonal optimization

1. Introduction

Currently, alarm regarding climate change and resource diminution issues are growing worldwide, especially in the tropical climate zones. The tropical region is famous with hot and humid climate conditions, and lies between the latitude of 15° south and 15° north, This region covers the areas of Malaysia, Philippines, Australia, Singapore, Indonesia, India, part of Africa, and Latin America [1]. The Tropics is considered as a region where human evolvement and comfort has often been taken for granted while the built environments are progressively becoming a public concern.

Solar radiation is a phenomenon that affects millions of people in tropical climate regions. The urbanization rate of developing countries like that in Malaysia is increasingly rising. This has led to the increasing effects of solar radiation in the cities, which leads to increased energy needs. The demand for comfort conditions in buildings has significantly increased as a result of exposure to an uncomfortable outdoor climate [2]. This has contributed to putting an enormous pressure on the cooling demand in the cities, and the local climate seriously disturbs the indoor thermal environment in buildings. In tropical climates, buildings absorb heat during the day due to solar irradiation heat gain through the building envelope. From a sustainable design point of view, it requires lowering the indoor daytime temperature below the outdoor temperature using building elements through passive or active systems. The residential sector has been identified as one of the major suppliers to the global environmental impact due to their high energy usage. Most developing countries continue to experience rapid growth in population and urbanization, and these countries

have shown a tremendous increase in energy consumption over the past three decades. For example, in Malaysia over the last two decades, the nationwide final energy demand has increased fivefold. In the past 30 years, the total population has doubled from 17.9 million in 1990 to 32.04 million in 2020. The Malaysian Government is implementing measures to cut wastage by enhancing energy sufficiency and efficiency. In this guideline, the government launched the National Green Technology Policy in August 2009. The objective of this policy was to provide a direction toward the management of a sustainable environment. Moreover, in 2010, Malaysia added 1.5 billion Ringgit ($360 million) to its budget to encourage green technology. Therefore, a key measure of environmental protection and energy management in Malaysia is to reduce energy use for space cooling in buildings [3]. It has been reported that the energy used by residential buildings can be reduced by more than 40% if the energy efficiency is well arranged and sustainable technologies are applied to the building envelope. Malaysia is a country located beside the Equator and experiences a similar climate of hot humid temperature throughout the year. Kuala Lumpur is the capital city of Malaysia, which has a population of 1.8 million in 2019, and is located at a latitude of 3.14 and longitude of 101.69, as shown in Figure 1. The typical climate of Kuala Lumpur has the characteristics of very small variation in monthly temperature [4]. The most crucial climatic effects in Kuala Lumpur buildings are the high intensity of solar irradiation and high-temperature of daily air.

Figure 1. Location of Kuala Lumpur. Source: World Atlas Travel.

Many researchers have already conducted studies from different angles on the effect of solar radiation. According to the length of the wave, solar radiation can be divided into different wavelength bands such as ultraviolet light, visible light, and near infrared light. The wavelength of ultraviolet light is less than 400 nm, accounting for about 5% of total solar energy. The visible light wavelength range is 400–760 nm, which accounts for about 45% of the total solar energy. The infrared wavelength is greater than 760 nm, accounting for about 50% of the total solar energy. It can be seen that solar energy is mainly concentrated in the visible and infrared regions, as shown in Figure 2.

A high-reflective material refers to a new material with a total reflectance or different solar radiation band reflectance higher than that of traditional external protective coatings. It is an effective material in a cool roof (exterior wall). At present, domestic and foreign scholars have carried out relevant research on high-reflective materials used in building envelopes, and have developed various high-reflective materials such as light-colored slurry seals, resin coatings, and water-based emulsion coatings. The rate ranges from 0.4 to 0.7, which greatly improves the reflectivity of the outer protective structure.

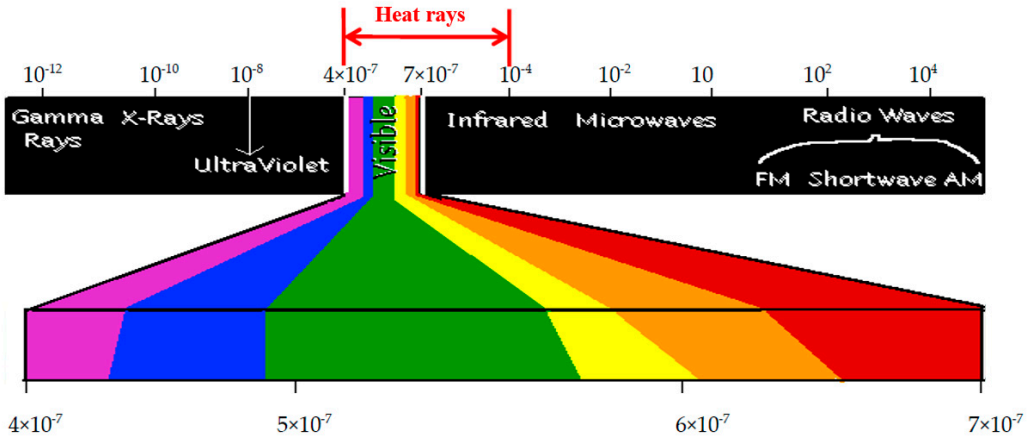

Figure 2. Solar heat ray emission spectrum.

This article is based on the current research, which through the combination of hollow glass beads and a nano-coating, coating pigment selection, and optimization of design composition, greatly improved its heat reflection efficiency and reduced brightness [5]. This material had a reflectance of over 93% and a hemispherical reflectance of 88%. The heat reflection ability of this material has been greatly improved, which is more in line with the energy-saving insulation requirements of buildings in tropical climate regions. The most innovative point is that the brightness of the coating was less than 50%, and the safety and comfort were greatly improved. A comparative analysis for two scenario models of a two-story residential building in Kuala Lumpur, Malaysia was conducted. This study examined the individual effect of different paints for an exterior wall on the building cooling load. The cooling effect will estimate and evaluate via comparison of the scenarios using the solar radiation analysis of Autodesk Revit plugging by integrating the data collected from Meteonorm [6]. This study combined environmental real-time data and building energy prediction modeling to understand the specific mechanisms of how high-reflective materials affect building energy consumption.

2. Materials and Methods

2.1. Selection of Fillers

We used imported solid acrylic resin as the base material, and used special materials such as "hollow beads" to form a high-performance reflective paint film. This kind of paint film not only has an anticorrosive and decorative function of industrial and architectural coatings, but also plays an excellent role in cooling and heat insulation [7]. The reflection ratio of hollow microbead filler to near infrared light is much higher than that of ordinary filler. The reflection ratio of glass microbeads and ceramic microbead sis similar, but the thermal insulation effect of ceramic microbeads is general and the storage stability is poor. In the process of filler comparison, the reflectance of the ordinary fillers, zinc oxide, cordierite, glass beads, and ceramic beads was 0.30, 0.45, 0.50, 0.88, and 0.89; among them, zinc oxide and ceramic beads had a thickening phenomenon, and other fillers did not change. Therefore, we selected hollow glass beads as the main filler. The reference formula (mass ratio) of insulating glass bead thermal insulation coating was: acrylic emulsion (50%):ethylene glycol monobutylether:hollow glass beads:distilled water:thickener = 20:0.8:35:25:25. In the test, we first tested the uncoated steel plate and the steel plate coated with a common coating. The results showed that the surface temperature of the uncoated steel plate was 81.1 °C, and the surface temperature of the steel plate coated with the common coating was 69.0 °C. Then, while keeping the other components unchanged, we used hollow glass microbeads, ceramic microbeads, cordierite, expanded perlite, sepiolite, and diatomaceous earth to replace the fillers in the common coating formula. The reflection and heat insulation effect of the coating was tested, and the coating surface temperatures were: hollow glass microbeads 55.8 °C;

ceramic beads 60.3 °C; cordierite 57.2 °C; expanded perlite 58.5 °C; sepiolite 58.3 °C; and diatomite 56.8 °C.

All kinds of fillers in the above have a certain reflection and heat insulation effect. Among them, the hollow glass microbeads had the best effect, and the surface temperature of the coating was only 55.8 °C, which was 13.2 °C lower than that of the common coating; the ceramic microbeads had the worst effect, and the surface temperature reached 60.3 °C, which was only 8.7 °C lower than that of the common coating. This may be related to the structural characteristics of the filler itself. Glass has a large refractive index. At the same time, because the hollow glass microbeads have a hollow structure, when light irradiates the surface of the coating, multiple reflections can be generated through the hollow glass microbeads, which improves the light reflection efficiency of the coating. However, other materials do not have this structure, so hollow glass microbeads have a good thermal insulation effect.

Based on the above results, we selected hollow glass microbeads as the research object. The mass fractions of the hollow glass microbeads were 10%, 15%, 20%, 25%, 30%, 35%, and 40%, and the film thickness was 300 μm. In this case, the reflective heat insulation effect of the coating was measured. It can be seen that when the content reached 35%, the glass microbeads were densely arranged on the surface of the coating and the reflectance to sunlight reached the maximum [8]. Continuing to increase the content of glass microbeads can only increase the thickness of the microbeads in the film, and has no effect on the arrangement density of the microbeads on the surface of the coating. Therefore, the reflective heat insulation effect of the film does not change obviously.

2.2. The Influence of Near-Infrared Nano-TiO_2 on the Properties of the Coating

Small size fillers have superior reflective properties, especially in the near-infrared region. This is due to the increase in the grain boundaries and crystal surface when fillers with small particle sizes aggregate, which can reflect more incident light. Therefore, nano-sized fillers have better optical reflection characteristics. The reflection ratio of hollow microbead fillers to near infrared light is much higher than that of ordinary fillers [9]. We mixed hollow glass microbeads with nano-TiO_2, and selected average 2-micron hollow glass microbeads as the main component, and the surface of the microbeads was coated with a 70–80 nanometer metal nano-coating with high reflectivity. The scanning electron microscope (SEM) images are shown in Figure 3a,b.

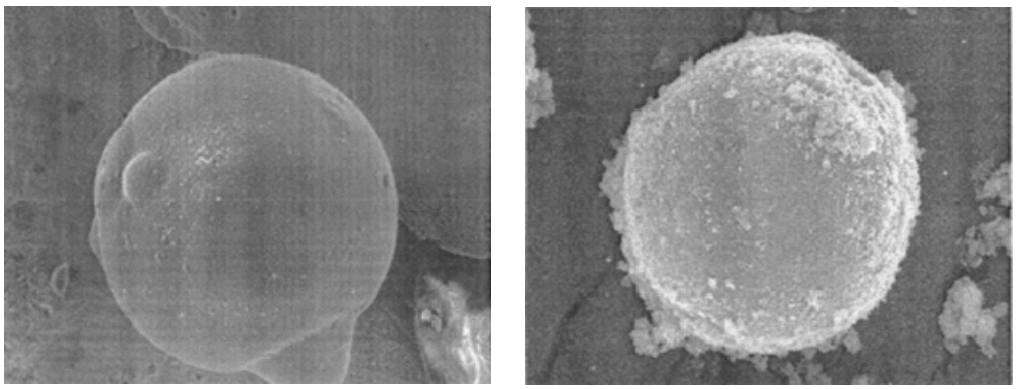

(**a**) (**b**)

Figure 3. (**a**) SEM images of hollow glass microbeads; (**b**) SEM images of hollow glass microbeads wrapped with nano-TiO_2.

With the increase in TiO_2 content, the total reflectance (Rtotal)/near infrared reflectance (Rnir) increased first and then decreased (stable), the visible light reflectance (Rvisi) decreased, and the ultraviolet light reflectance (Ruv) hardly changed. The test results are shown in Figure 4. In the chromaticity space, as the mass fraction of TiO_2 increased, the brightness coefficient L* decreased, and the red and green channel index a* increased first and then decreased, indicating that the hiding power decreased first and then increased; that is, the darkest/hiding power reached its lowest at

10%. Therefore, we used 10% as the central point and set the level of near-infrared titanium dioxide (NIR-TiO_2) in the orthogonal experiment to 3%, 5%, and 10%. The results showed that the amount of near-infrared titanium dioxide was less than 10% in engineering application, as shown in Figure 4.

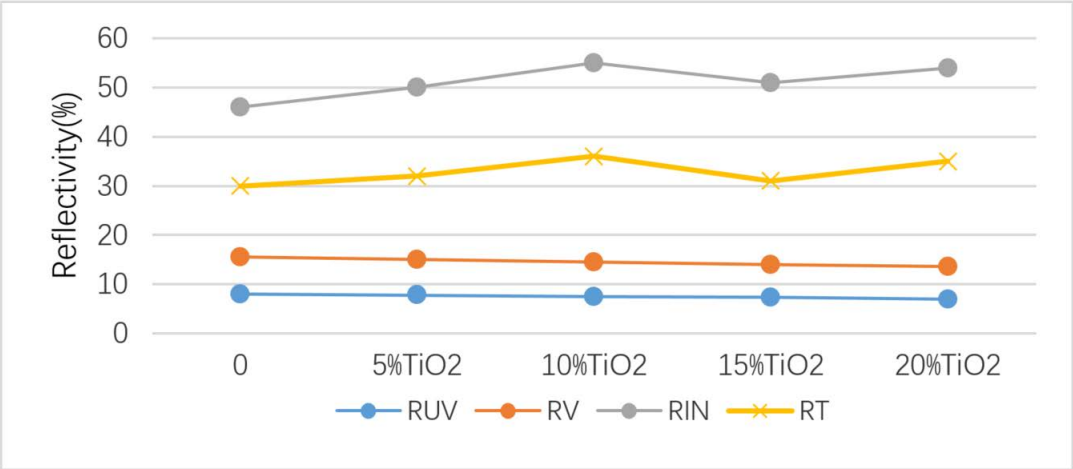

Figure 4. Effect of near infrared NIR-TiO_2 on the reflectivity of the coating in different wavebands.

2.3. Selection of Pigments Based on Safety and Comfortable Visual Characteristics

In addition to the particle size of the filler, the color also has a greater effect on the optical reflection characteristics of the filler [10]. We tested the optical reflection characteristics of different color fillers, and the results are shown in Figure 5. Yellow, green, and red fillers are more recommended as reflective fillers while for black fillers, the blending amount must be controlled and can be mixed with other colors.

In particular, high reflectivity of buildings in the tropics will lead to high requirements for the visual safety of buildings, that is, excessive reflectivity will cause glare. We established a quantitative model between the optical reflection characteristics of the coating and the brightness index. The linear relationship between the visible light reflectance and the brightness index exhibited an exponential relationship. When the coating was a medium and low brightness ($40 < L^* < 80$), as the brightness increased, the visible light reflectance of the coating increased linearly; when the coating was high brightness ($L^* > 80$), as the brightness increase, the dark light reflectance of the coating increased exponentially [11]. Therefore, when optimizing the design of the coating, it is better to control the visible light reflectance of the coating to below 50% in order to control the brightness. Therefore, we chose iron oxide red color, which is more appropriate. From the perspective of the chromaticity space brightness index (L^*), iron oxide red is a low-brightness, high-reflectivity filler, has excellent optical reflection characteristics, and can be a functional filler for dark high-reflection coatings.

The reflectance characteristics of red resin coating included a reflectivity between 28.7%–40.4% and had a high near-infrared light reflectivity ranging from 38.8% to 55.8%. Titanium dioxide and red iron oxide can improve the reflectivity of the coating. The total reflectance of the white resin coating containing only titanium dioxide could reach 62.6%, and the near infrared reflectance could reach 67.7%. For iron oxide red with small particle sizes as a functional filler, when the mass fraction is the same, its density is lower, the volume is larger, and the hiding power is stronger [12]. Therefore, the incorporation of small-diameter iron oxide red obviously improved the reflectivity of the coating, reduced the brightness, and helped to achieve a "cool dark" coating.

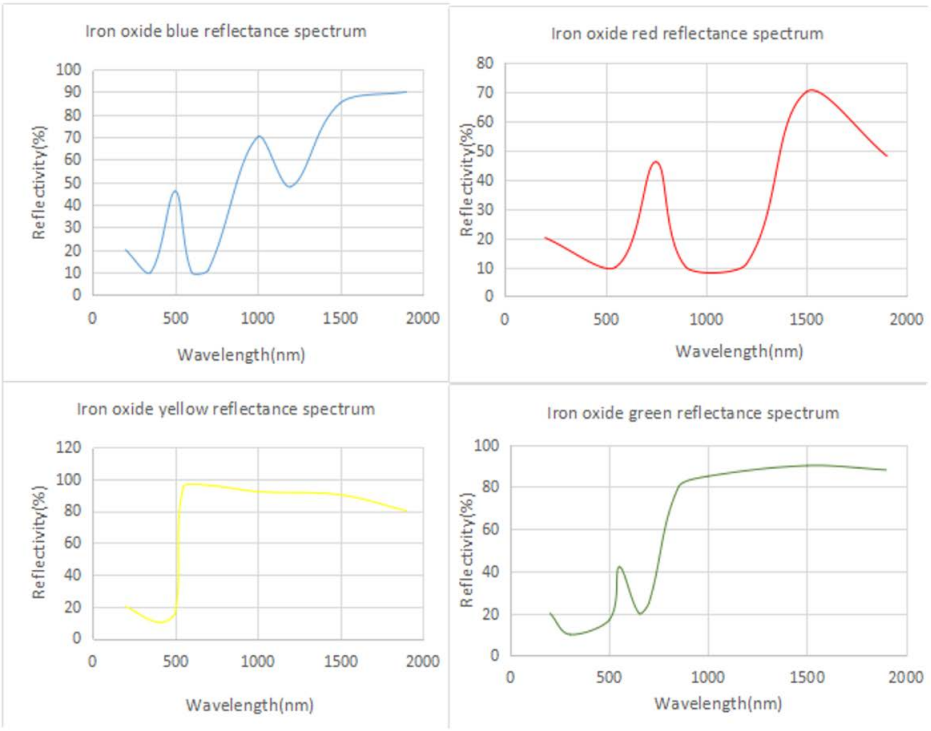

Figure 5. Full spectrum reflectance of different filler powders (200–2500 nm).

2.4. *Preparation of Low-Brightness and High-Reflective Coatings*

2.4.1. Experimental Materials and Instruments

Raw materials: hollow glass beads, water-based epoxy resin emulsion, titanium dioxide (nano-titanium dioxide), iron oxide red, additives, etc.

Instruments: High-speed dispersion machine: JJ-1 (Jiangsu Jintan Ronghua Instrument Manufacturing Co., Ltd., Changzhou, Jiangsu, China); tensile strength test: CMT 6104 Universal Electronic tensile testing machine (Shenzhen Century Tianyuan Instrument Co., Ltd., Shenzhen, China), refer to the standard GB/T 528-1998; Thermal insulation temperature difference test: The device is in accordance with JG/T 235-2008 "Building reflective insulation coating materials" standard self-made, test reference standard JG/T 235-2008, thermal insulation temperature difference [13]. The test device is shown in Figure 6.

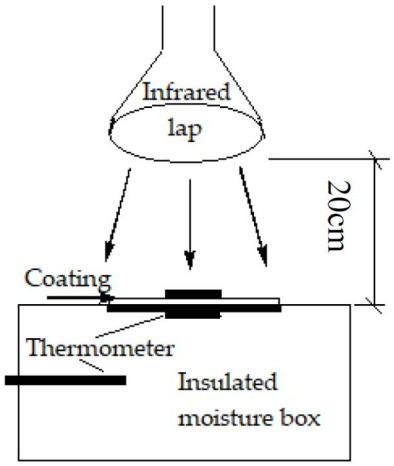

Figure 6. Schematic diagram of the self-made reflective insulation effect measuring device.

2.4.2. Design of Comprehensive Packing Formula Based on Orthogonal Experiment

According to the above analysis results, we can refer to the basic formula of thermal insulation coatings and make appropriate fine-tuning to obtain the basic formula of coatings: Water accounted for 5.23%; waterborne epoxy resin emulsion accounted for 53.54%; additives accounted for 6.23%; and filler accounted for 35.00%.

We used the comprehensive balance method to carry out orthogonal experimental analysis on the optimal composition of the filler, as shown in Table 1. In order to optimize the coating formula and achieve the best ratio between the pigments and fillers, we used the method of orthogonal experiment to analyze the primary and secondary relationships and the optimal matching conditions of each influencing factor [14]. On the basis of previous experiments, we listed rutile titanium dioxide, hollow glass beads, and iron oxide red as the three elements. Hollow glass beads are a mixture of hollow beads with different particle sizes in proportion. There are three indicators in the formula: total reflectance (Rtotal), near infrared reflectance (Rnir), and chromaticity spatial brightness index (L*), which have three levels respectively. We conducted an experimental analysis to find the best formula.

Table 1. Level table of the pigment and filler orthogonal test factors.

Level	Rutile Titanium Dioxide/g	Hollow Glass Beads/g	Iron Oxide Red/g
1	6	8	2
2	8	10	4
3	10	12	6

2.4.3. Preparation and Testing of Coatings

There are two common methods of coating preparation: the colored paste method and dry coloring method. The color paste method refers to the method of mixing pigments, fillers, additives, and solvents in a certain proportion, grinding them into a high-concentration slurry, and then dispersing and mixing with the resin in a certain proportion, and finally adjusting the stiffness and preparing the coating. The dry coloring method is a preparation method in which all pigments, fillers, and solvents are directly added to the base material in proportion, and directly ground or dispersed to a suitable drilling degree [15]. In this experiment, the dry coloring method was used to mix the epoxy resin emulsion, reflective heat insulation pigments and fillers, additives, and solvents, and after high-speed dispersion in a high-speed dispersing machine, a curing agent was added in a certain proportion and fully stirred to prepare the heat reflective insulation coating. In the experiment, it should be noted that the hollow glass beads are light, brittle, and easy to break, so they cannot be ground and stirred at high speed.

First, the additives and fillers were dispersed into water one by one under high-speed stirring, and stirred for 30 min to prepare a slurry. Then, the emulsion was slowly added to the slurry under the condition of medium-speed stirring. After the addition, stirring continued 30 r/min to obtain the coating. Brush the prepared coating on a stainless steel plate into a coating film with a diameter of 15 cm and a thickness of 650 μm, and the reflective heat insulation coating film was obtained after being completely dried for 24 h. According to Table 2, a total of seven coating films were obtained. Since the reflection brightness of the 7, 8, and 9 coating films was tested to exceed 50%, they were discarded. Samples 1–7 of the preparation coating film is shown in Figure 7.

Table 2. Orthogonal experimental scheme of the coating filler formula and coating performance.

Number	Rutile Titanium Dioxide/g	Hollow Glass Beads/g	Iron Oxide Red/g	Surface Temperature of Coating Film/°C	Total Reflectance Rtotal/%	Near Infrared Reflectance Rnir/%	Brightness L* (≤50%)
1	6	8	2	59.6	76.2	87.3	0.37
2	6	10	4	59.4	77.8	88.4	0.42
3	6	12	6	59.1	80.5	90.3	0.48
4	8	8	4	59.2	79.8	89.6	0.38
5	8	10	6	58.9	81.3	91.3	0.43
6	8	12	2	58.6	82.1	92.1	0.45
7	10	8	6	59.3	78.5	89.0	0.51
8	10	10	2	58.8	80.4	91.7	0.53
9	10	12	4	58.9	80.8	91.4	0.50
K1	59.37	59.37	59.08	-	-	-	-
K2	58.94	59.03	59.16	-	-	-	-
K3	59.00	58.97	59.10	-	-	-	-
R	0.39	0.41	0.11	-	-	-	-

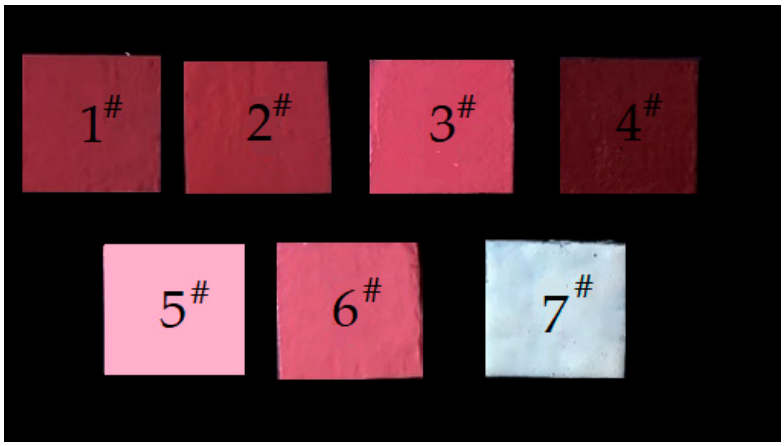

Figure 7. Coating photos.

3. Results and Discussion

In a closed environment laboratory that maintains an indoor ambient temperature of 25 °C, the tested sample plate in the hollow at the top of the thermal insulation box was placed, and we used an infrared lamp to simulate the sun light source at a distance of 20 cm directly above for 30 min, as shown in Figure 8. That is, a stable thermal equilibrium state was reached. At this time, the temperature of the upper surface of the coating film, the temperature of the back surface of the steel plate and the ambient temperature of the box are measured, and the upper surface temperature is used as the main reference value for the reflection and heat insulation effect of the coating film.

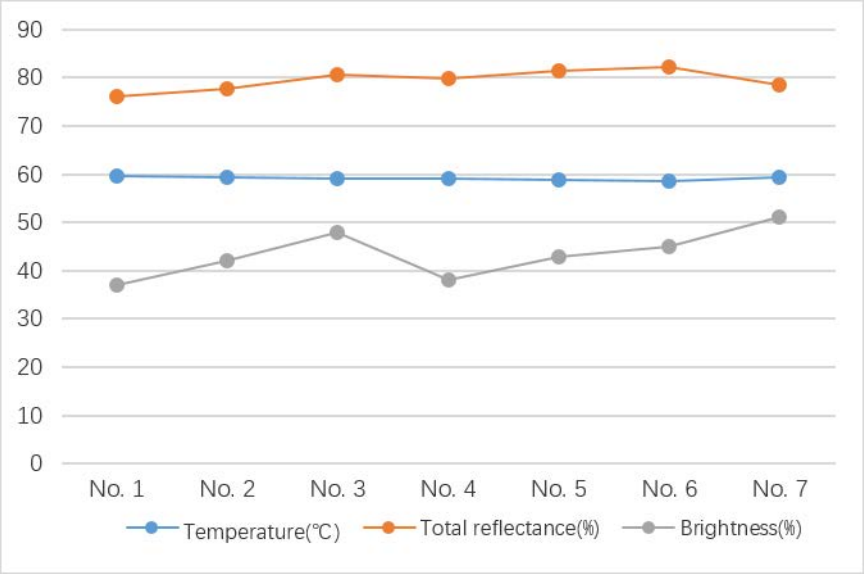

Figure 8. Box diagram of the temperature distribution of the coating sample.

Based on the above test methods, we tested the coating temperature, reflectivity, and brightness, and seven parallel samples were used for each coating. The results are listed in Table 2. It can be seen from Table 2 that the primary and secondary order of the various factors that affect the comprehensive index is: C (iron oxide red) > A (TiO_2) > B (hollow glass beads). Among them, the coating film of 6 had the lowest surface temperature, the highest reflectivity, and the brightness L* ≤ 50%. The coating formulas of 7, 8, and 9 were discarded because of L* > 50%. Therefore, the sixth group of filler formulas were used, namely: rutile titanium dioxide:hollow glass beads:iron oxide red = 8:12:2.

4. Application and Conclusions

4.1. Application

The methodology implemented in this paper was based on an analytical literature study and comparative analysis work for the two scenarios model of two stories of a residential building in Kuala Lumpur, Malaysia, as shown in Figure 9a,b. We conducted a simulation analysis on the application of the low-brightness and high-reflective coatings for this residential building. Table 3 shows the thermal characteristics of the materials used in the simulated residential building. Figure 9a,b shows the application of ordinary coatings and low brightness and high reflection coatings, respectively.

To carry out the thermal behavior analysis, two types of software, namely Autodesk Revit 2016 and Meteonorm 7.1.3 were used to perform the simulation. The solar radiation plugging tool in Autodesk Revit 2016 was used for the simulation. This plugging tool is an ideal tool suitable for the analysis of complex and expandable models and can easily accomplish all simulation requirements, which can be integrated into the building design process. This software is capable of calculating an accurate thermal behavior analysis at any time [16]. Meteonorm generates and stores weather data using a stochastic method. Data stored in Meteonorm are taken from 8300 weather stations placed worldwide. The data consist of hourly wet and dry bulb temperatures, relative humidity, wind speed, and cloud cover [17]. Autodesk Revit architecture generated the thermal properties of the materials been used in this project, where the solar radiation package in Revit performed the solar irradiation calculations on the external surfaces of the building. In this paper, Meteonorm was used to generate outdoor hourly air temperature in Kuala Lumpur, Malaysia to compare the solar irradiation analysis plugging in Autodesk Revit.

(**a**) (**b**)

Figure 9. (**a**) Two story residential building with common coatings. (**b**) Two story residential building with low-brightness and high-reflective coatings.

Table 3. Thermophysical parameters of the building used for simulation.

Function	Material	Thickness (cm)	Density kg/m^3	Specific Heat J/(g·°C)	Thermal Conductivity w/(m·k)	R-Values (m^2·k)/w	U-Values w/(m^2·k)
Roof	Paper	0.5	930	1.30	0.04	0.13	0.48
	Plaster	4.5	1600	1.09	0.22	0.20	
	EPS	5.0	50	1.20	0.03	1.67	
	Concrete cast	15.0	1200	1.00	1.40	0.11	
Window	Glass	0.6	2700	0.84	0.80	0.01	3.25
	UPVC frames	7.5	510	1.35	0.25	0.30	
Wall	Plaster	5.0	1600	1.09	0.22	0.23	0.49
	Concrete block	20.0	1800	0.84	1.30	0.15	
	EPS	5.0	50	1.20	0.03	1.67	

The simulation was conducted on April 11, 2019. The selected day was chosen due to Kuala Lumpur's hottest season, which starts from March up to the first half of May. The simulation consists of three main stages, where only two of them were considered as the coatings' effect. The simulation included three main parts, namely the east wall, the west wall, and the roof. The roof part receives the largest amount of solar radiation, so the coating effect is the most obvious. For the simulation of the solar irradiation roof, the time interval was from 10:00 to 15:00, and the coating effect is shown in Figure 10. In the same way, the reflectivity and thermal characteristics of the east and west walls can be obtained. Adding this kind of coating film, in the same way, the reflectivity and thermal characteristics of the east and west walls can be obtained.

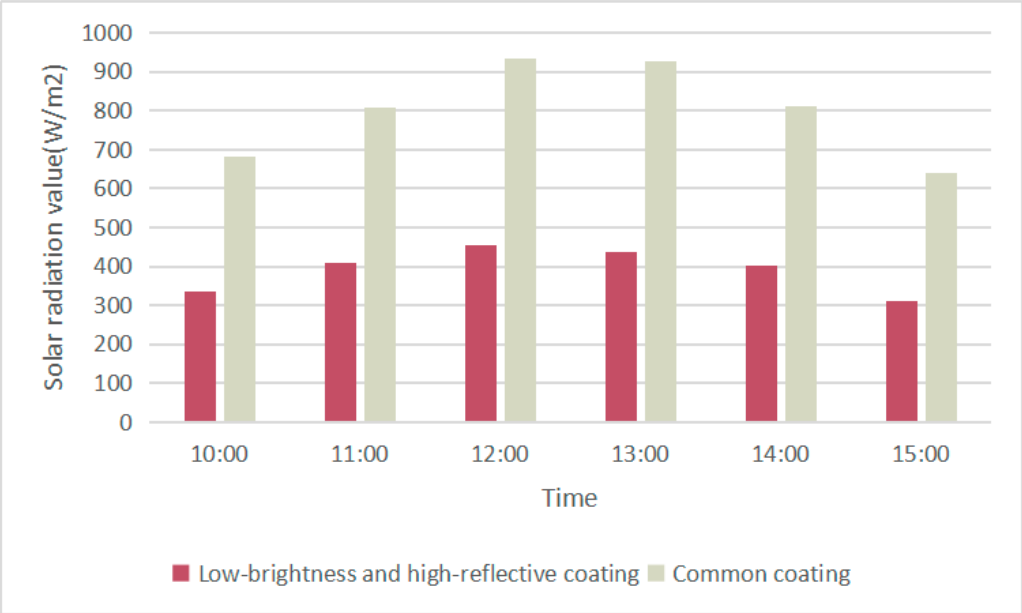

Figure 10. Solar irradiation values on the roof.

The results obtained from our simulation showed that the roof reduced the maximum solar irradiation most, followed by the east and the west surfaces represented as 47.9%, 32.5%, and 21.6%, respectively. The results indicated that the heat reflective insulation coating could reduce the exterior envelope surface temperature effectively, and the maximum temperature change is about 8–10 °C. As shown in Table 4, the standard model simulation calculation results show that when the reflectance of the outer protective structure coating increased from 7% to 92.1%, the annual energy saving rate of this multi-story building was 12.9%. The annual air-conditioning electricity saving with the coating was about 6.7 kWh/(m^2·year), which shows that the energy saving effect of the heat insulation coating is obvious in Kuala Lumpur. Our findings revealed that low-brightness and high-reflective coatings gradually reduced the energy consumption for cooling [18,19]. At the same time, the brightness of the coating was less than 50%, and its comfort and safety met the requirements.

Table 4. Energy consumption simulation results.

Near Infrared Reflectance	7%	14.4%	34%	53%	65%	80%	92.1%
Annual energy Consumption kWh/m^2a	50.0	49.5	48.3	46.9	45.8	44.2	43.3

4.2. Conclusions

This paper studied a low-brightness, high-reflection coating suitable for tropical areas with high solar radiation. This coating has the characteristics of low brightness and high reflectivity. We carried out the coating application effect research on a small residential building in Kuala Lumpur, Malaysia. Through the research, we can draw the following conclusions:

(1) Hollow glass microspheres exhibit good light reflection ability due to their structural characteristics, and are an excellent heat insulating filler.

(2) The reflective and thermal insulation effect of the coating will increase with the increase of the thermal insulation filler content, but when the thermal insulation filler content reaches 35%, the reflective thermal insulation effect will reach the maximum value [20]. Continuing to increase the content of the thermal insulation filler will not affect the reflection thermal insulation effect.

(3) The combination of hollow glass microspheres and nano-titanium dioxide shows a better reflective and heat-insulating effect than using a heat-insulating filler alone. The best filler ratio was rutile titanium dioxide:hollow glass beads: ron oxide red = 8:12:2.

(4) The reflective and thermal insulation effect of the coating is strengthened with the increase of the coating film thickness, but when the coating film thickness reached 550 μm, the reflective thermal insulation effect reached the maximum, the coating film thickness continued to increase, and the reflective thermal insulation effect no longer changed.

(5) The influence of resin on the heat insulation effect is very limited.

(6) Considering the driving safety and the visual characteristics of personnel, too high a reflectivity will cause glare. When optimizing the design of the coating, the visible light reflectance of the coating should be controlled below 50% to control the brightness of the coating. The incorporation of iron oxide red with a small particle size can significantly increase the reflectivity of the coating, while reducing the brightness, which helps to achieve a "cool dark" coating.

The results of this study showed an excellent solution for building exterior thermal insulation under climatic conditions in tropical hot and high radiation areas. However, more detailed and comprehensive research is needed to confirm this solution in future studies.

Author Contributions: Conceptualization, X.R. and L.J.; methodology, X.K.; validation, X.R., L.J., and X.K.; formal analysis, X.K.; investigation, G.Y.; data curation, X.K. and L.J.; writing—original draft preparation, L.J.; writing—review and editing, L.J. and G.Y.; visualization, X.K.; project administration, X.K. All authors have read and agreed to the published version of the manuscript.

Funding: This research was funded by Hebei Provincial Transport Department Project, grant number QG2018-3.

Conflicts of Interest: The author has no conflict of interest. The funders had no role in the design of the study; in the collection, analyses, or interpretation of data; in the writing of the manuscript, or in the decision to publish the results.

References

1. Jamaludin, N.; Khamidi, M.F.; Wahab, S.N.; Klufallah, M.M. Indoor Thermal Environment in Tropical Climate Residential Building. In *E3S Web of Conferences*; EDP Sciences: Wuhan, China, 2014; Volume 3, p. 01026.
2. Ahmed, K.S. Comfort in urban spaces: Defining the boundaries of outdoor thermal comfort for the tropical urban environments. *Energy Build.* **2003**, *35*, 103–110. [CrossRef]
3. Rajapaksha, I.; Nagai, H.; Okumiya, M. A ventilated courtyard as a passive cooling strategy in the warm humid tropics. *Renew. Energy* **2003**, *28*, 1755–1778. [CrossRef]
4. Hsieh, C.M.; Li, J.J.; Zhang, L.; Schwegler, B. Effects of coatings and transpiration on building cooling energy use. *Energy Build.* **2018**, *159*, 382–397. [CrossRef]
5. Santamouris, M.; Synnefa, A.; Karlessi, T. Using advanced cool materials in the urban built environment to mitigate heat islands and improve thermal comfort conditions. *Solar Energy* **2011**, *85*, 3085–3102. [CrossRef]
6. Al-Tamimi, N.A.M.; Syed Fadzil, S.F. Thermal performance analysis for ventilated and unventilated glazed rooms in Malaysia (comparing simulated and field data). *Indoor Built Environ.* **2011**, *20*, 534–542. [CrossRef]
7. Shi, N.N.; Tsai, C.C.; Camino, F.; Bernard, G.D.; Yu, N.; Wehner, R. Keeping cool: Enhanced optical reflection and radiative heat dissipation in Saharan silver ants. *Science* **2015**, *349*, 298–301. [CrossRef] [PubMed]
8. Howell, J.R.; Menguc, M.P.; Siegel, R. *Thermal Radiation Heat Transfer*; CRC Press: Boca Raton, FL, USA, 2015.
9. Bribián, I.Z.; Usón, A.A.; Scarpellini, S. Life cycle assessment in buildings: State-of-the-art and simplified LCA methodology as a complement for building certification. *Build. Environ.* **2009**, *44*, 2510–2520. [CrossRef]
10. Arto, I.; Capellán-Pérez, I.; Lago, R.; Bueno, G.; Bermejo, R. The energy requirements of a developed world. *Energy Sustain. Dev.* **2016**, *33*, 1–13. [CrossRef]
11. Xie, N.; Li, H.; Abdelhady, A.; Harvey, J. Laboratorial investigation on optical and thermal properties of cool pavement nano-coatings for urban heat island mitigation. *Build. Environ.* **2019**, *147*, 231–240. [CrossRef]
12. Abdel-Aziz, D.M.; Al Shboul, A.; Al-Kurdi, N.Y. Effects of coatings on Building's Energy Consumption-The Case of Residential Buildings in a Mediterranean Climate. *Am. J. Environ. Eng.* **2015**, *5*, 131–140.
13. ASHRAE, S. *Standard 189.1-2014 Standard for the Design of High-performance Green Buildings. American Society of Heating, Refrigerating, and Air-Conditioning Engineers*; ASHRAE: Atlanta, GA, USA, 2014.

14. Joshi, N.; Joshi, A. Role of Urban Trees in Amelioration of Temperatures. *Int. J. Res. Stud. Biosci.* **2015**, *3*, 132–137.
15. Jackson, E.A. Naturalistic Play Environments: Activating Children's Ecological Awareness, Development and Senses through Natural Materials. Master's Thesis, Washington State University, Pullman, WA, USA, 2009.
16. Stine, D. Building Performance Analysis in Revit 2016 R2 with Autodesk Insight 360. 2015. Available online: http://aecbytes.com/tipsandtricks/2015/issue76-revit.html (accessed on 12 August 2019).
17. Remund, J. Accuracy of Meteonorm 7. A Detailed Look at the Model Steps and Uncertainties. 2015. Available online: http://www.meteonorm.com/images/uploads/downloads/Accuracy_of_Meteonorm_7.pdf (accessed on 21 April 2016).
18. Hassid, S.; Santamouris, M.N.; Papanikolaou, N.; Linardi, A.; Klitsikas, N.; Georgakis, C.; Assimakopoulos, D.N. The effect of the Athens heat island on air conditioning load. *Energy Build.* **2000**, *32*, 131–141. [CrossRef]
19. Ong, W.J.; Tan, L.L.; Chai, S.P.; Yong, S.T.; Mohamed, A.R. Facet-Dependent Photocatalytic Properties of TiO_2-Based Composites for Energy Conversion and Environmental Remediation. *ChemSusChem.* **2014**, *7*, 690–719. [CrossRef]
20. Akbari, H. Shade trees reduce building energy use and CO_2 emissions from power plants. *Environ. Pollut.* **2002**, *116*, S119–S126. [CrossRef]